WEATHER RESEARCH IN-SITU FIELD CAMPAIGN OVER THE ATACAMA DESERT

Ricardo Fonseca
María-Paz Zorzano
Armando Azua-Bustos
Carlos González-Silva
Javier Martín-Torres

UNIVERSIDAD DE TARAPACÁ
ARICA - CHILE

CENTRO DE ASTROBIOLOGÍA
ASOCIADO AL NASA ASTROBIOLOGY INSTITUTE

GOBIERNO DE ESPAÑA · CSIC Consejo Superior de Investigaciones Científicas · INTA Instituto Nacional de Técnica Aeroespacial

Coastal and Environmental Sensing And Modeling (CESAM) Laboratory

LULEÅ UNIVERSITY OF TECHNOLOGY

Khalifa University جامعة خليفة

DUBAI FUTURE FOUNDATION مؤسسة دبي للمستقبل

IPM

DUC IN ALTUM · UA · UNIVERSIDAD AUTONOMA DE CHILE

IACT
INSTITUTO ANDALUZ DE CIENCIAS DE LA TIERRA

1. Numerical Model

The Weather Research and Forecasting (WRF; Skamarok et al., 2008) model version 3.9.1.1 is used to dynamically downscale the 0.5° × 0.5° National Centers for Environmental Prediction Climate Forecast System Reanalysis (CFSR; Saha et al., 2010) data over Atacama desert, for two week-long periods in the austral winter season (30th June - 6th July 2018; 15th - 23rd August 2018). WRF is run in a four-nested configuration (spatial resolutions of 27, 9, 3 and 1 km) with 60 levels in the vertical, concentrated in the Planetary Boundary Layer (PBL). The output of the 1 km grid is post-processed and stored every 10 min, and then used for analysis. Further details about the experimental set up are given in Fonseca et al. (2019).

The physics parameterization schemes employed are shown in the table below:

Physics Options	Parameterization Scheme
Microphysics	Goddard (six-class) Cloud Microphysics Scheme
Radiation	Rapid Radiative Transfer Model for GCM Applications (RRTMG)
Surface Layer	Revised MM5 Monin-Obukhov Scheme
Land Surface	Noah Land Surface Model
Planetary Boundary Layer	Yonsei University (YSU) PBL scheme
Cumulus *(27 km and 9 km grids only)*	Modified Betts-Miller-Janjić (BMJ) Scheme (Fonseca et al., 2015) + Precipitating Convective Cloud (PCC) Scheme (Koh et al., 2016)
Sea Surface Temperature	CFSR SST + simple skin temperature scheme (Zeng et al., 2005)

The two figures on the left show the model grids (spatial resolutions of 27 – 9 – 3 – 1 km) and the spatial extent and orography of the 1 km grid, with the location of the three sites considered in this study given. The last figure on the right is a view at the location of site #3. These sites were selected for an aerobiology study, presented in Azua-Bustos et al. (2019).

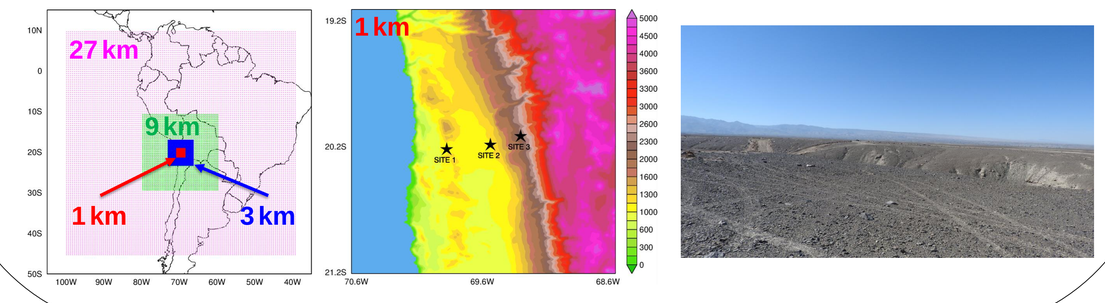

2. Sensitivity Experiments

- The figures below show surface temperature (°C) and relative humidity (RH; %) at location of site #1, for the three-day period 30th June – 2nd July 2018. The black curve shows the observed values, and the blue curve the WRF predictions with the default settings. WRF overestimates observed surface temperature in particular during daytime, with biases in excess of 10°C.
- In order to improve the agreement between model predictions and observations, the albedo was increased by 15%. This is justified, as the albedo used in WRF has a 10-15% relative accuracy (Csiszar and Gutman, 1999). However, the impact was found to be rather small, with a reduction in daytime surface temperature of 0.5-1°C. Given the strong dependence of surface temperature on soil properties, tunable parameters in the soil model of the Noah Land Surface Model (LSM), defined in the file "SOILPARM.TBL", are perturbed. The soil texture at the three sites is loam.

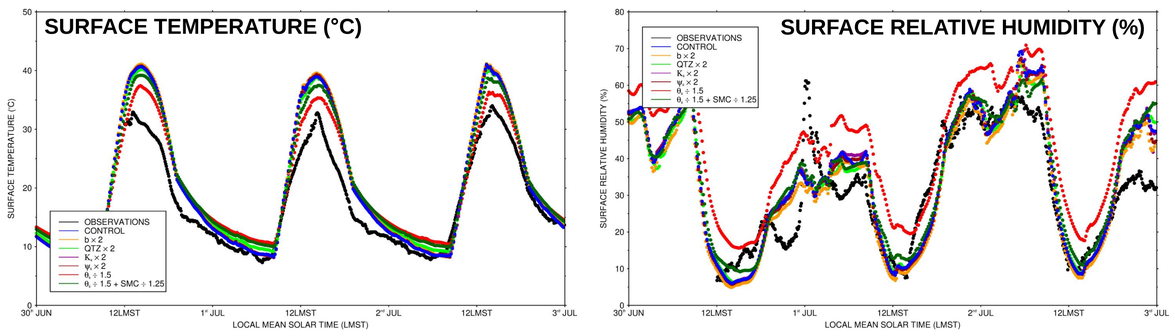

- There are five tunable parameters in the soil model used in Noah LSM:
  - ✓ **Soil porosity, θ_s**. A reduction in soil porosity leads to a less porous/more compact soil, which will have a higher thermal inertia, giving higher nighttime and lower daytime temperatures;
  - ✓ **Soil suction, ψ_s**. Measure of the potential of the soil above the water table to attract water. A higher ψ_s will increase the soil's thermal inertia;
  - ✓ **Saturated soil hydraulic conductivity, K_s**. A soil with higher K_s will also have higher thermal inertia, so increasing K_s may help in reducing the daytime warm bias in WRF;
  - ✓ **Quartz Fraction, QTZ**. A higher quartz fraction will increase the soil thermal inertia, as quartz has significantly larger thermal conductivity compared to the other minerals in the soil;
  - ✓ **b parameter**. Empirical parameter that depends on soil texture and controls the soil hydraulic properties. A higher value of the b parameter also leads to a higher soil thermal inertia.
- The orange, light green, purple, brown and red curves show the model's response to a change in the referred five parameters. The one that gives the largest sensitivity is the soil porosity. While a reduction in θ_s by one-third does alleviate the daytime temperature biases, the nighttime temperatures are now much warmer than observations, also with higher relative humidities;
- One way to correct for excessive RH is to reduce the soil moisture content (SMC), read in from CFSR. The dark green curve shows response to a reduced θ_s and soil moisture content by one third and one fifth, respectively. While the RH values are in closer agreement with observations, the drier soil and resulting lower thermal inertia leads to higher daytime surface temperatures;
- A "perfect" agreement between model predictions and observations cannot be obtained simply by perturbing the tunable parameters in soil model of Noah LSM or surface albedo. A possible explanation is the lack of a groundwater table in the Noah LSM (Fei Chen, *pers. comm.*), which can be rather shallow in arid regions, including in the Atacama Desert (McKay et al., 2003);
- A simulation is conducted with the Noah scheme with multiparameterization options (Noah-MP), which includes, among other things, a groundwater model. However, the daytime temperature is still overestimated by the model. It is concluded that an optimized version of Noah LSM (or Noah-MP) has to be developed for arid/desert regions, or a more sophisticated version of WRF, such as WRF-HYDRO, has to be employed, for a correct simulation of the surface fields.

3. Evaluation of WRF performance

- Figures below show observed and model-predicted surface temperature (°C) and RH (%) for the three sites for 30th June – 6th July 2018. The blue curve shows model predictions with default settings, while the red curve shows WRF forecasts when the soil tunable parameters and SMC are perturbed in the following way: $b \times 2$; $\theta_S \times (1.7 \div 3)$; $\psi_S \times 2$; $K_s \times 2$; $QTZ \times 2$; $SMC \div 1.5$. The panels below show the model bias;
- For all sites, WRF overestimates daytime surface temperature by up to 11°C. At night, biases for sites #1 and 2 are of a smaller magnitude, but at site #3 they are negative and comparable to daytime biases. For sites #1 and 2, the WRF biases match those reported by Gunwani and Mohan (2017) over arid regions in India, while for site #3 they may attributed to a drier soil or incorrect setting of soil properties such as θ_s. The RH is well simulated at site #1, but at sites #2 and 3, in particular at site #3, it is largely overestimated at night, by up to 35%. Pozo et al. (2016) reported that WRF tends to overpredict the near-surface water vapour mixing ratio over the high terrain in the Andes;
- By and large, the WRF predictions are more skillful when soil properties are updated. For example, at site #1, the RH is better captured, and the colder nighttime temperatures are partially corrected. At site #3, the temperature predictions are also more accurate. Despite these improvements, however, large biases are still present, in particular in the daytime surface temperature, and for site #3 in the RH.

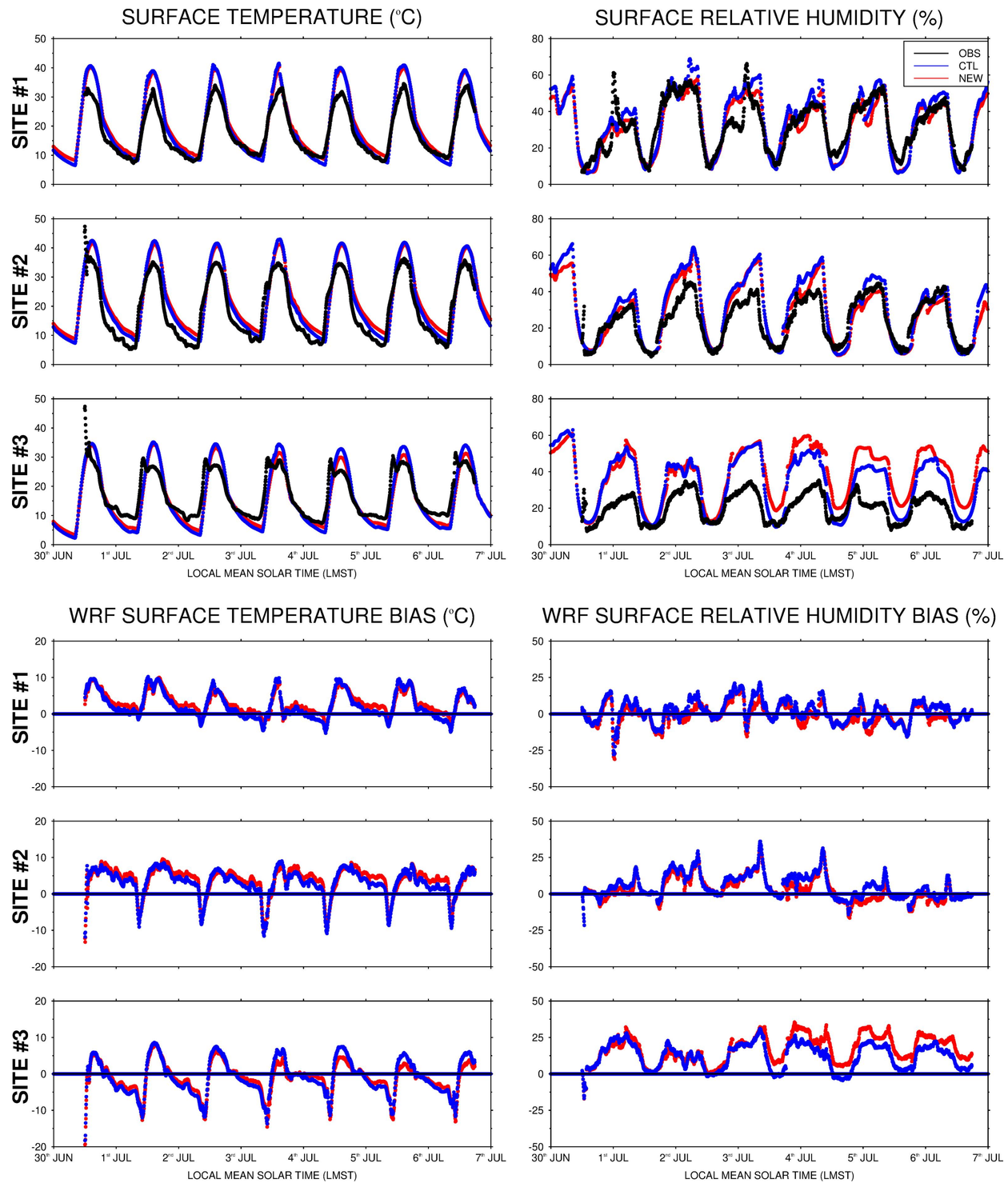

- The table below shows the WRF surface temperature biases, at the location of each site and for the two periods considered, with respect to in-situ measurements and estimates from the Moderate Resolution Imaging Spectroradiometer (MODIS; Wan, 1996) payload imaging sensors', product MOD11C1. While at night the biases with respect to the two sources are comparable, during daytime they are very different. For example, for site #1 and the first period, the WRF daytime temperature is colder by about 2.4°C with respect to MODIS, and is warmer by 5°C with respect to the in-situ measurements. In the second period, the differences are even larger: for site #1, MODIS underestimates the surface temperature by 17°C;
- There are two main reasons for the discrepancy between the MODIS and in-situ temperature estimates: (i) the very large difference between air and surface temperature in hyperarid regions like the Atacama Desert, which can exceed 16°C, the upper-limit used in the MODIS algorithm, and (ii) large errors in the surface emissivity values in MODIS bands 31 and 32, estimated from land cover types (Li et al., 2014);
- It is concluded that there is a need for a comprehensive network of ground-based weather sensors in remote regions such as the Atacama Desert, where satellite-derived products can have significant biases and hence cannot be trusted for model evaluation and calibration.

WRF Bias		MODIS (daytime)	Ground Sensors (daytime)	MODIS (nighttime)	Ground Sensors (nighttime)
SITE 1	30/06 - 06/07	-2.4ºC	+5.0ºC	+3.3ºC	+1.7ºC
	15/08 - 23/08	-10.6ºC	+6.8ºC	+4.9ºC	+4.7ºC
SITE 2	30/06 - 06/07	-1.6ºC	+3.5ºC	+6.0ºC	+4.5ºC
	15/08 - 23/08	-5.1ºC	-0.3ºC	+7.5ºC	+6.5ºC
SITE 3	30/06 - 06/07	-0.8ºC	+0.4ºC	-1.0ºC	-1.8ºC
	15/08 - 23/08	-4.5ºC	+0.7ºC	+1.4ºC	+0.1ºC

References

Azua-Bustos, A., Gonzalez-Silva, C., Fernandez-Martinez, M., Arenas-Fajardo, C., Fonseca, R., Martin-Torres, F. J., Fernandez-Sampedro, M., Fairen, A. G., Zorzano, M.-P., 2019: Aeolian transport of viable microbial life across the Atacama Desert, Chile: Implications for Mars. *Sci. Rep.*, **9**, 110224, doi:10.1038/s41598-019-47394-z

Csizar, F. and G. Gutman, 1999: Mapping the global land surface albedo from NOAA/AVHRR. *J. Geophys. Res.*, **104**, 6215-6228.

Fonseca, R.M., Zhang, T., and T.-Y. Koh, 2015: Improved Simulation of Precipitation in the Tropics in WRF using a Modified BMJ Scheme. *Geosci. Model Dev.*, **8**, 2915-2928.

Fonseca, R.M., Zorzano-Mier, M.-P., Azua-Bustos, A., González-Silva, C., Martin-Torres, J., 2019: A surface temperature and moisture intercomparison study of the Weather Research and Forecasting Model, in-situ measurements and satellite observations over the Atacama Desert. *Q. J. R. Meteorol. Soc.*, **145**, 2202-2220.

Gunwani, P. and M. Mohan, 2017: Sensitivity of WRF model estimates to various PBL parameterizations in different climatic zones over India. *Atmos. Res.*, **194**, 43-65.

Koh, T.-Y. and R.M. Fonseca, 2016: Subgrid-scale Cloud-Radiation Feedback For the Betts-Miller-Janjić Convection Scheme. *Q. J. R. Meteorol. Soc.*, **142**, 989-1006.

Li, H. and Coauthors, 2014: Evaluation of the VIIRS and MODIS LST products in an arid area of Northwest China. *Remote Sens. Environ.*, **142**, 111-121.

McKay, C.P. and Coauthors, 2003: Temperature and moisture conditions for life in the extreme arid region of the Atacama Desert: four years of observations including the El Niño of 1997-1998. *Astrobiol.*, **3**, 393-406.

Pozo, D. and Coauthors, 2016: Validation of WRF forecasts for the Chajnantor region. *Mon. Not. R. Astron. Soc.*, **459**, 419-426.

Saha, S. and Coauthors, 2010: The NCEP Climate Forecast System Reanalysis. *Bull. Amer. Meteor. Soc.*, **91**, 1015–1057.

Skamarock, W. C and Coauthors, 2008: A description of the Advanced Research WRF version 3. NCAR tech. Note TN-4175_STR, 113pp.

Wan, Z., 1996: A generalized split-window algorithm for retrieving land-surface temperature from space. *IEEE Trans. Geosci. Remote Sens.*, **34**, 892-905.

Zeng, X. and Beljaars, A., 2005: A prognostic scheme of sea surface skin temperature for modeling and data assimilation. *Geophys. Res. Lett.*, **32**, L14605, doi:10.1029/2005GL023030.